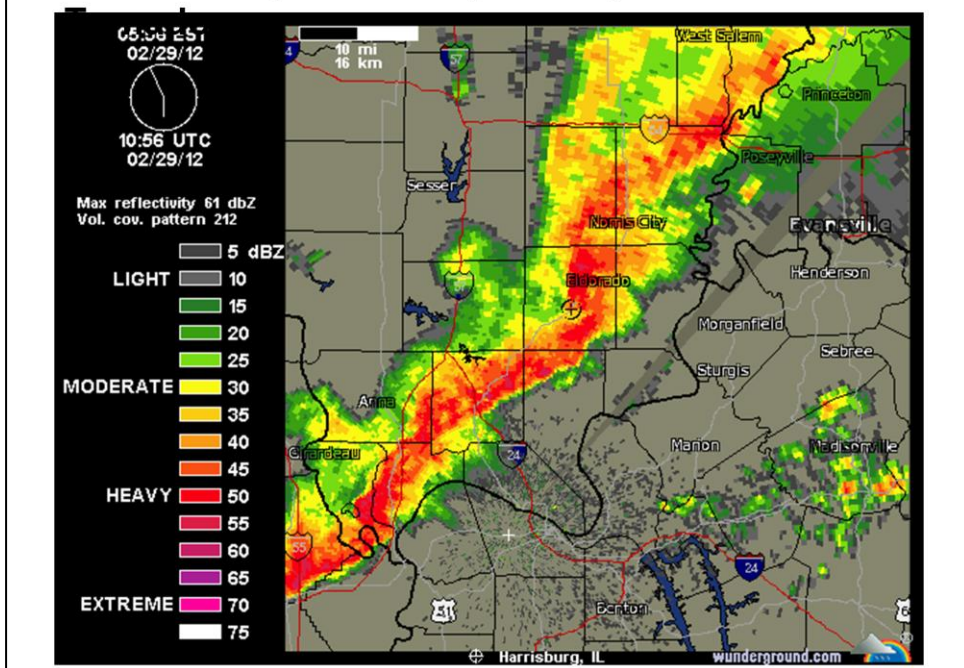
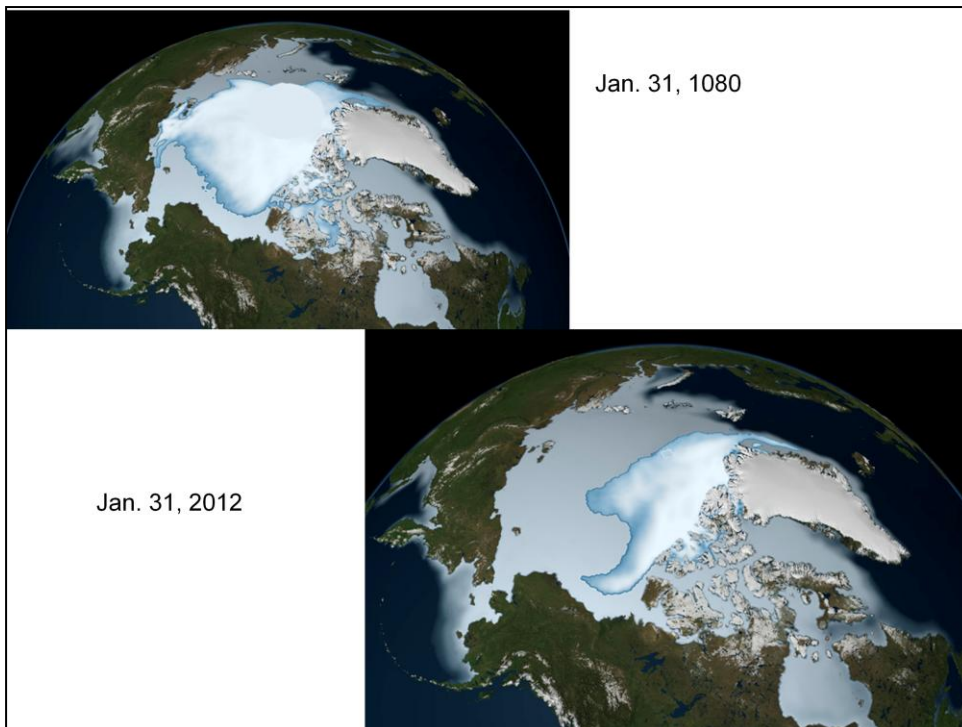


# 800-Mile Supercell Drops Multiple





A new study by NASA scientist [Joey Comiso](#) has found that the oldest and thickest Arctic sea ice is disappearing at a faster rate than the younger and thinner ice at the edges of the ice cap. The rapid disappearance of older ice makes the Arctic Ocean's sea ice cap more vulnerable to further decline.

Overall Arctic sea ice “extent”—which includes all areas where at least 15 percent of the ocean surface is covered by ice—has been vanishing at a rate of  $-15.1$  percent per decade, Comiso found. Over the same period, the area covered by multi-year ice has been shrinking by  $-17.2$  percent per decade. The findings were published in February 2012 in the [Journal of Climate](#).

The images above show sea ice coverage in 1980 and 2012, as observed by passive microwave sensors on NASA’s [Nimbus-7](#) satellite and by the [Special Sensor Microwave Imager/Sounder \(SSMIS\)](#) from the Defense Meteorological Satellite Program (DMSP). Multi-year ice is shown in bright white, while average sea ice cover is shown in light blue to milky white. The data shows the ice cover for the period of November 1 through January 31 in their respective years.

The thickest “multi-year” ice survives through two or more summers, while young, seasonal ice forms over a winter and typically melts just as quickly as it formed. Scientists also describe a third category: “perennial” ice is all ice cover that has survived at least one summer. All multi-year ice is perennial ice, but not all perennial ice is multi-year ice.

Comiso found that perennial ice extent has been shrinking at a rate of  $-12.2$  percent per decade, while its area is declining at a rate of  $-13.5$  percent per decade. These numbers indicate that multiyear ice is declining faster than the perennial ice that surrounds it.

As perennial ice has retreated over the past three decades, it has opened up new areas of the Arctic Ocean that could then be covered by seasonal ice. A larger volume of seasonal ice meant that a larger portion of it could make it through the summer to form second-year ice. This is likely the reason why the perennial ice cover, which includes second year ice, is not declining as rapidly as multiyear ice cover, Comiso said.

“The Arctic sea ice cover is getting thinner because it’s rapidly losing its thick component,” Comiso said. “At the same time, the surface temperature in the Arctic is going up, which results in a shorter ice-forming season. It would take a persistent cold spell for multi-year sea ice to grow thick enough again to be able to survive the summer melt season and reverse the trend.”

### **Further Reading**

Comiso, Josefino C. (2012, February) [Large Decadal Decline of the Arctic Multiyear Ice Cover](#). *Journal of Climate* 25, 1176–1193.

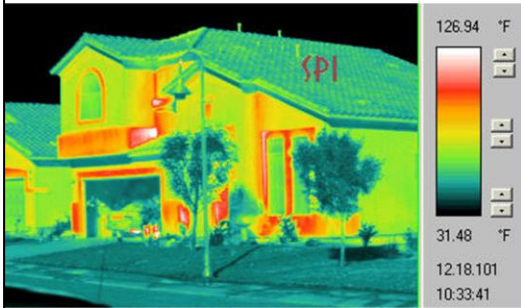
NASA (2012, February 29) [NASA Finds Thickest Parts of Arctic Ice Cap Melting Faster](#).

NASA Earth Observatory (n.d.) [World of Change: Arctic Sea Ice](#).

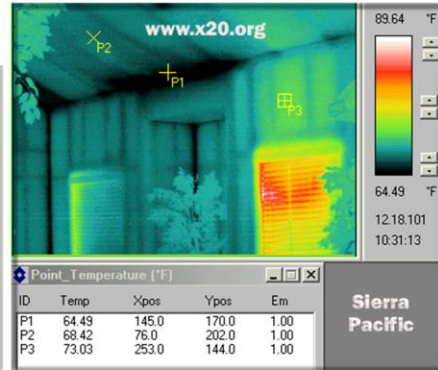
Image by the NASA Scientific Visualization Studio based on data from the Special Sensor Microwave Imager/Sounder (SSMIS) of the Defense Meteorological Satellite Program (DMSP). Caption based on a story by Maria-José Viñas, NASA Earth Science News Team.

Instrument: DMSP - SSM/I

Lecture 16 03/01/2012 Chapter 13, 10  
 Urban Remote Sensing  
 Heat islands  
 Impervious surfaces and hydrology  
 High Spatial Resolution  
**Spectral Mixture Methods**



Thermal Infrared image of a residential home



Thermal image of a residential home; black indicates poor/missing insulation, Temperatures at P1, P2, and P3 are shown

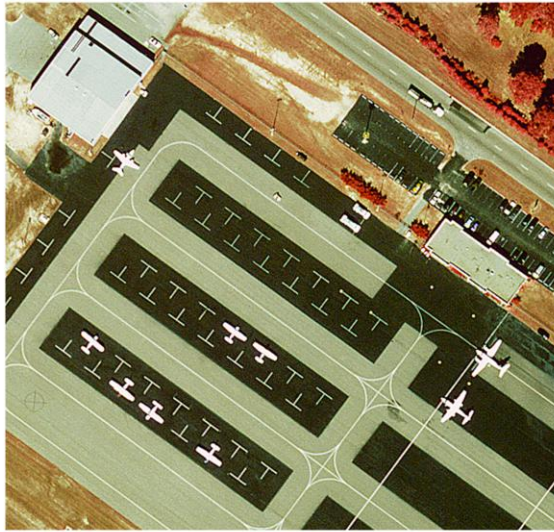


Thermal scans of a house before, left, and after being insulated. In Britain, subsidies cover much of the cost of home insulation.

## Uses of Urban Remote Sensing

- Zoning regulation
- Commerce and economic development
- Tax assessment
- Transportation and utilities
- Parks, recreation, and tourism
- Emergency management
- Real Estate Developers

## Types of Information Acquired for Urban Studies



Airport Structures

What is the need here? Mostly spatial detail but spectral resolution helps also. It is what kind of image?

**IKONOS Panchromatic**



**Panchromatic Sharpened  
Near-infrared**



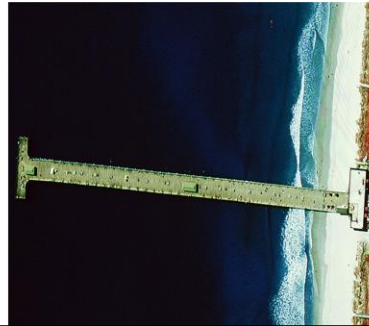
Columbia, SC on October 15, 2000

What do you see with Near infrared that you didn't see in the Pan alone?

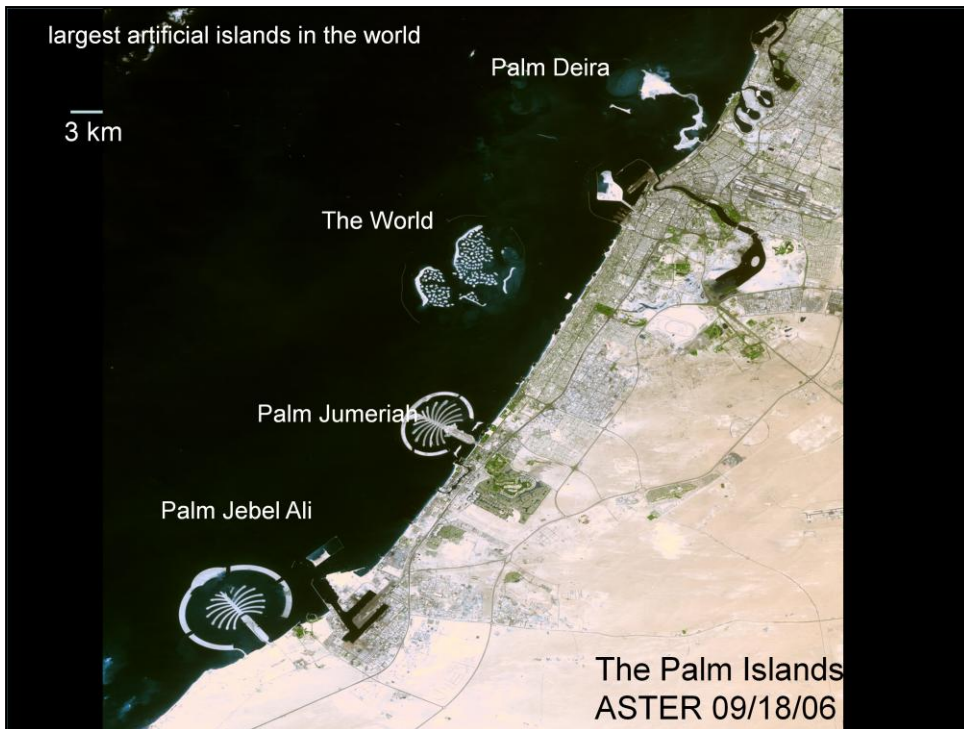


### Imaging Water Infrastructure:

Bridges,  
Piers,  
Locks



Clearly, high spatial resolution data is key to these observations



When the Advanced Spaceborne Thermal Emission and Reflection Radiometer ([ASTER](#)) on NASA's [Terra](#) satellite took this picture on September 18, 2006, these islands were the largest artificial islands in the world. All of the islands were still under some degree of [construction](#) in the fall of 2006.

Urban Housing: Type, Density, Surroundings, Roads & Streets



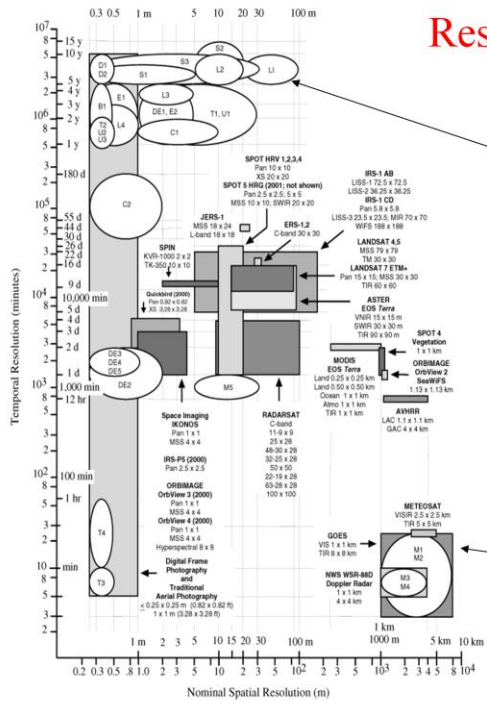


Do you recognize this area in Davis? The green, Village Homes

# Resolution Requirements

Clear polygons represent the spatial and temporal characteristics of selected *urban attributes*

Gray boxes depict the spatial and temporal characteristics of the *remote sensing systems* that may be used to extract the required urban information



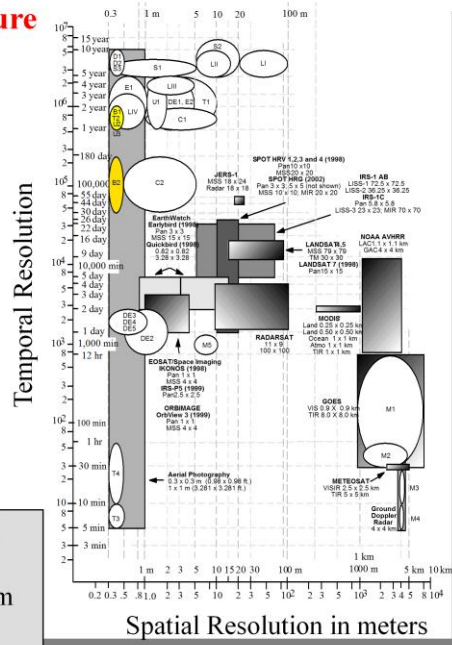
# Building and Cadastral (Property Line) Infrastructure



Derived from  
0.3 x 0.3 m  
(1 x 1 ft.)  
spatial  
resolution  
stereoscopic,  
panchromatic  
aerial  
photography



	Temporal	Spatial
B1 - building perimeter, area, volume, height	1 - 2 years	0.3 - 0.5 m
B2 - cadastral mapping (property lines)	1 - 6 mo	0.3 - 0.5 m

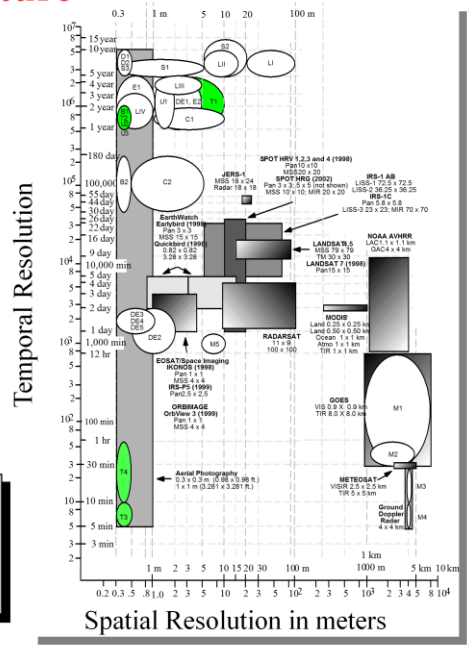


# Transportation Infrastructure



Irmo, S.C. TIGER road network updated using SPOT 10 x 10 m data

	Temporal	Spatial
T1 - general road Centerline	1 - 5 years	1 - 10 m
T2 - precise road width	1 - 2 years	0.3 - 0.5 m
T3 - traffic count studies (cars, planes etc.)	5 - 10 min	0.3 - 0.5 m
T4 - parking studies	10 - 60 min	0.3 - 0.5 m

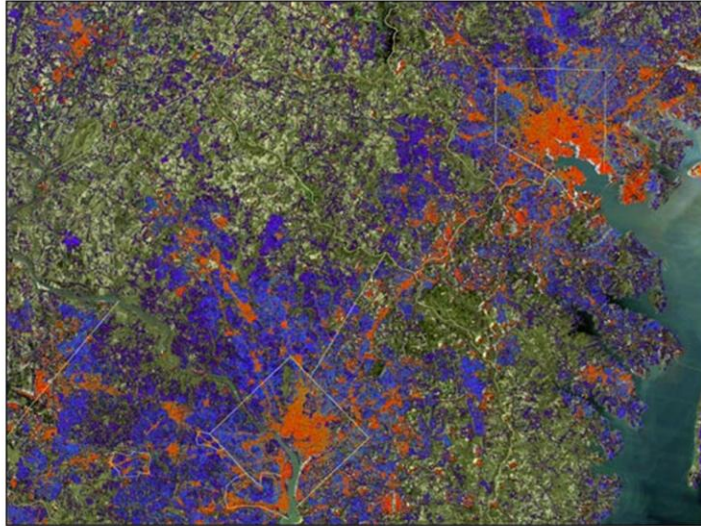


## Washington DC-Baltimore Area Impervious Surface

### Concentration of impervious Surfaces

Impacts:  
runoff,  
storm drainage,  
groundwater recharge,  
erosion,  
pollution

- High (20-40%)
- Medium (20-30%)
- Low 0-20%



Merged Landsat and IKONOS data (Andrew Smith)

Scientists are using a major advance in satellite-based land surface mapping to create more accurate and detailed city maps. These maps provide urban planners with a better understanding of city growth and how rainfall runoff over paved surfaces impact regional water quality.

These space-based maps of buildings and paved surfaces, such as roads and parking lots, which are impervious to water, can indicate where large amounts of storm water runs off. Concentrated runoff leads to erosion and elevated discharge of soil and chemicals into rivers, streams, and ground water.

Andrew Smith, a faculty research assistant at the Mid-Atlantic Regional Earth Science Applications Center produced a map of the Washington-Baltimore area that quantifies how much impervious surface there is across the entire region. Baltimore and the counties that border it have at least 20 percent, and up to 40 percent, impervious surface area, indicating that pollution from runoff could be a problem. The District of Columbia and surrounding watersheds in Virginia and Maryland have levels of impervious surfaces between 20 percent and 30 percent. Areas between and beyond the Baltimore-Washington corridor are more "green" with levels that range from 0 percent to 20 percent impervious surface areas.

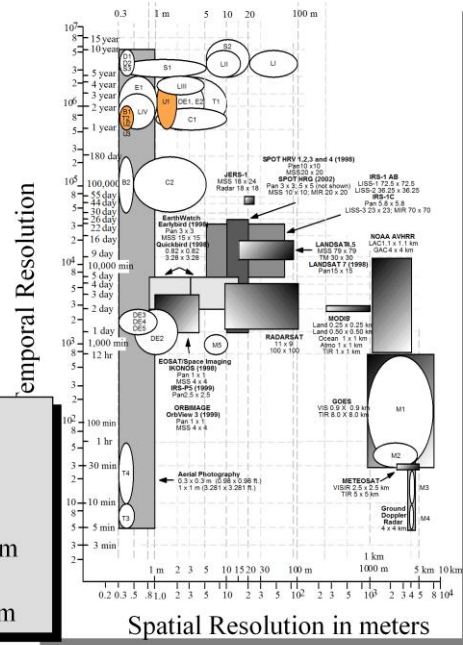
The image above shows the extent of impervious surfaces in and around Washington and Baltimore. Red represents high concentrations of impervious surfaces. Blue represents moderate concentrations and green represents low concentrations of impervious surfaces. The base image was acquired by NASA's Landsat satellite, while the map of impervious surfaces was derived with data from both Landsat and Space Imaging's high-resolution **IKONOS satellite**.

For more information, read: [New Satellite Maps Provide Planners Improved Urban Sprawl Insight](#)

# Utility Infrastructure



	Temporal	Spatial
U1 - general utility centerline	1 - 5 years	1 - 2 m
U2 - precise utility line width	1 - 2 years	0.3 - 0.6 m
U3 - locate poles, manholes, substations	1 - 2 years	0.3 - 0.6 m



# Disaster Emergency Response

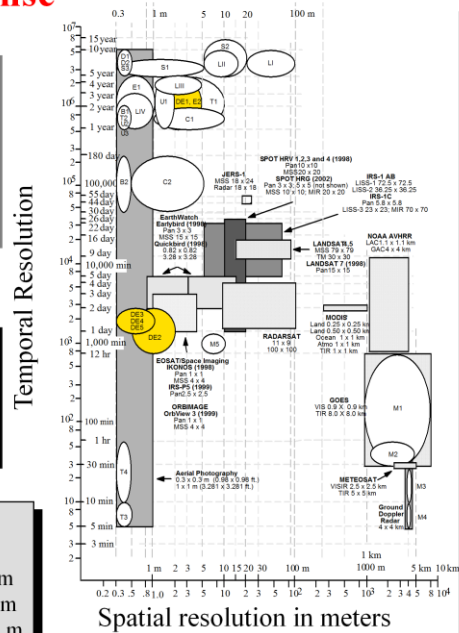


Pre-Hurricane  
Hugo  
Sullivan's Is.,  
S.C.  
July 15, 1988  
1 x 1 m  
panchromatic



Post-Hurricane  
Hugo  
Oct. 23, 1989  
1 x 1 m  
panchromatic

	Temporal	Spatial
DE1 - pre-emergency image	1 - 5 years	1 - 5 m
DE2 - post-emergency imagery	12 hr - 2 days	0.5 - 2 m
DE3 - damaged housing stock	1 - 2 days	0.3 - 1m
DE4 - damaged transportation	1 - 2 days	0.3 - 1 m
DE5 - damaged utilities	1 - 2 days	0.3 - 1 m

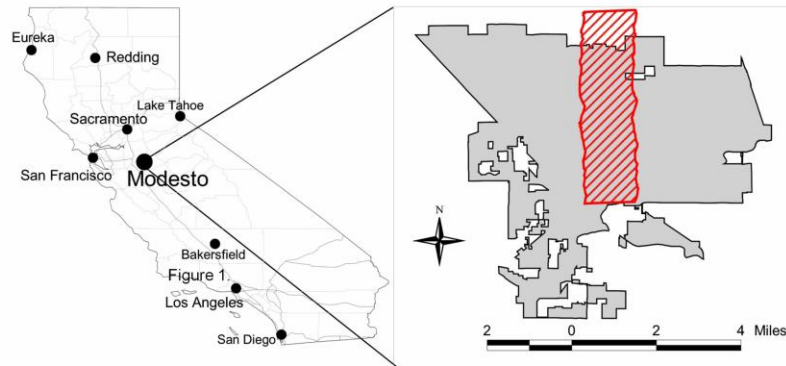




Space Imaging Inc. quickly provided two IKONOS images of the New York scene, one taken before the event and the second within a day after the horrific destruction of these, and several adjacent, buildings. Compare these two views, which illustrate the capability of space imagery to provide an overview of a disaster in an urban center:

On Saturday, September 15, after much of the smoke and dust was cleared by a heavy rain, IKONOS captured this 1-meter resolution image (a bit degraded in this rendition) of the World Trade Center devastation and the avenues filled with rescue and recovery vehicles:

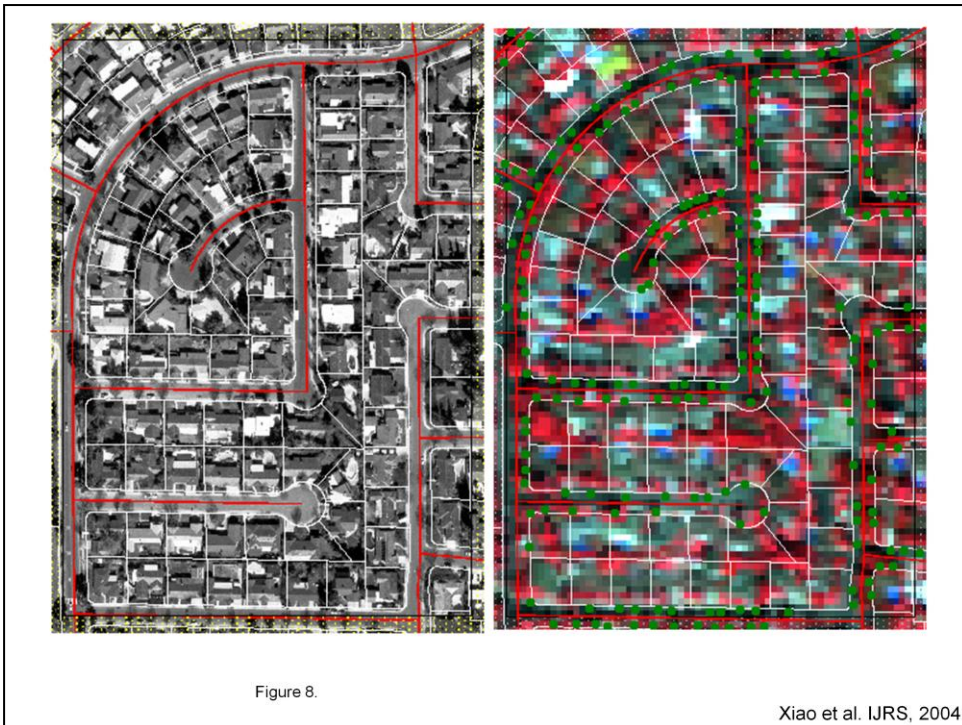
## Mapping Street Tree Species in Cities



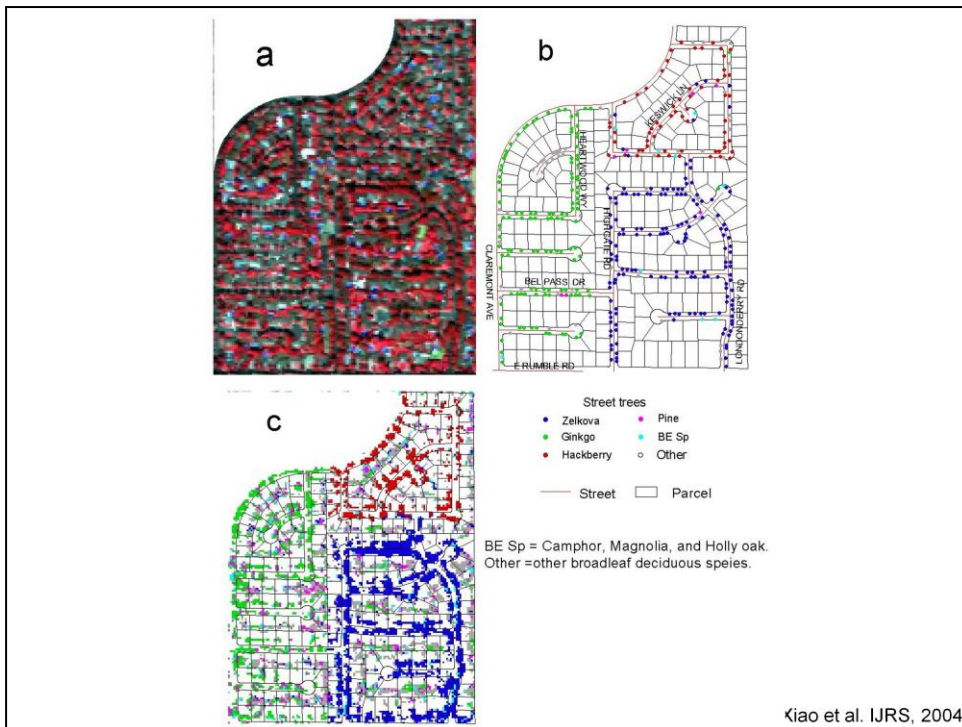
Xiao et al. IJRS, 2004

The increase in the proportion of pavement area during the process of urbanization strongly influences energy exchange, hydrology, and micro-climate. Many problems facing management of the urban ecosystem are related to these factors. For example, urban heat island effects and increased storm runoff are related to the imperviousness of pavement and buildings. Air quality and water use are related to crown density and tree density because the total leaf surface area and leaf surface area per units land area controls both air pollutants removal and evapotranspiration rates. Understanding impacts on air quality, energy partitioning, and hydrologic processes in the urban ecosystem depend on knowledge of tree species, leaf and stem surface areas, tree dimensions, and percentage of pavement cover, among other things. To understand how urban forests function and to estimate the value of their environmental services we must first recognize properties related to urban forest structure and composition. Also, a good understanding of the structure of the urban forest provides other information useful for urban managers, such as for planning tree pruning, removal, and insect or disease control activities.

The Modesto citywide street tree database contains 184 tree species and 75,629 individual trees. Most trees are broadleaf deciduous (87%) and the broadleaf evergreen and conifer tree types only account for 7% and 6%, respectively. Information for each tree includes: species code, scientific name and common name, tree ID number, year tree planted, and the access address (e.g. street address, city area, corner street, and corner address). The tree layer in GIS is generated from tree survey spreadsheet and the trees street address and street GIS layer based on the address matching method.



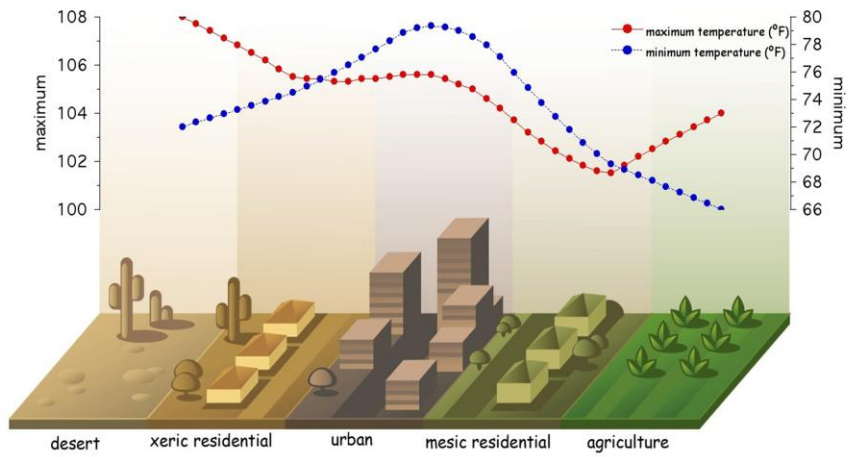
Aerial Photo and 4m CIR image allows identification of tree location but not tree type. High spatial resolution hyperspectral images have more information to identify individual species.



### Tree distribution in a subset of image area

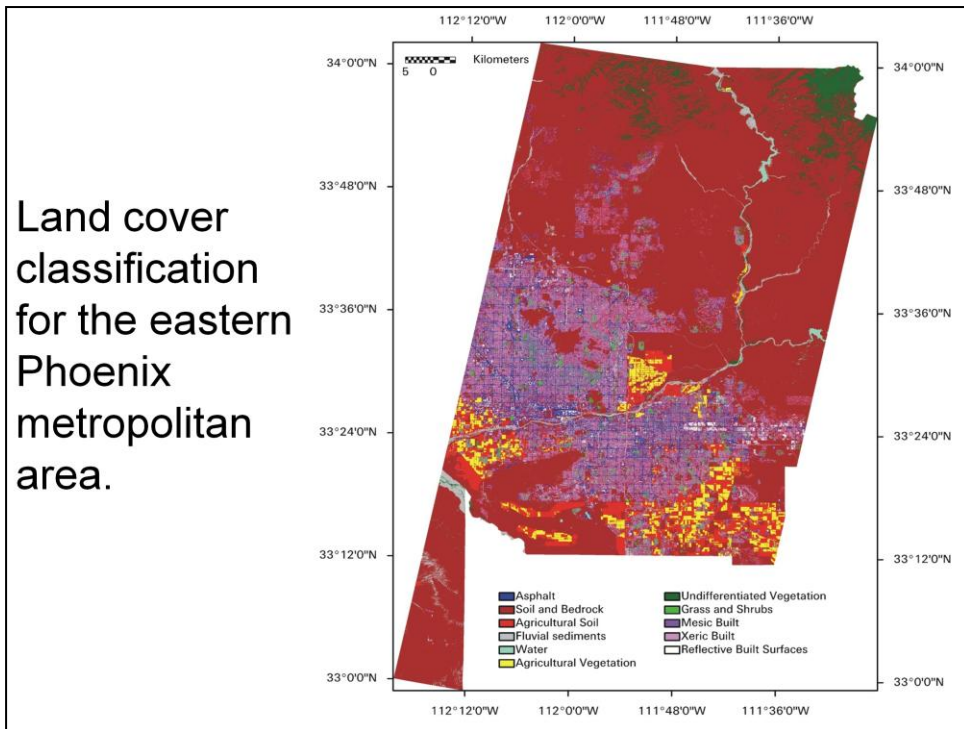
At the tree type level, mapping achieved 94% accuracy for the entire area. At the tree species level, the average accuracy was 70% but this varied with both tree type and species. For four evergreen tree species, the average accuracy was 69%. For 12 deciduous tree species, the average accuracy was 70%. The relatively low accuracy for several deciduous species was due to (1) small tree sizes and (2) overlaps among tree crowns at the 4m spatial resolution of AVIRIS data and (3) indistinct or inappropriate library spectra.

# Urban Heat Island



The heat island is a nighttime phenomenon in semi-arid regions.  
Residential and agricultural irrigation mitigate the heat island during the day.  
(Zehnder 2004)

Land cover classification for the eastern Phoenix metropolitan area.



The Urban Environmental Monitoring (UEM) project at Arizona State University was initiated by ASTER Team Member Philip R. Christensen to collect daytime and nighttime ASTER data over 100 urban centers twice per year (to capture local winter and summer seasons). The original objective was to provide baseline observations of the physical state of 100 cities beginning in 2000 (following the launch of the Terra satellite). This objective is being met by production of land cover classifications for each city using a modification of the expert system of Stefanov et al. (2001b) to construct a global baseline dataset to compare land cover changes during the duration of the Terra mission (nominally six years; Ramsey et al., 1999; Stefanov et al., 2001a; Ramsey, 2003). Unforeseen difficulties with the ASTER data acquisition scheduling algorithm, which accords low priority to urban acquisition targets, has resulted in incomplete coverage and sampling of the original 100 cities.

Brazel, A.J., N.Selover, R. Vose, and G. Heisler, The tale of two climates: Baltimore and Phoenix LTER sites. *Climate Research*, 15, pp. 123-135, 2000.

Grimm, N.B., J.M. Grove, C.L. Redman, and S.T.A. Pickett, Integrated approaches to long-term studies of urban ecological systems. *BioScience*, 70, pp. 571-584, 2000.

Haff, P.K., Neogeomorphology. *EOS Transactions*, 83 (29), p. 310, p. 317, 2002.

Netzband, M., and W.L. Stefanov, Assessment of urban spatial variation using ASTER data. *The International Archives of the Photogrammetry, Remote Sensing, and Spatial Information Sciences*, 34 (7/W9), pp. 138-143, 2003.

Ramsey, M. S., Mapping the city landscape from space: The Advanced Spaceborne Thermal Emission and Reflectance Radiometer (ASTER) Urban Environmental Monitoring Program, in Heiken, G., Fakundiny, R., and J. Sutter (eds.), *Earth Science in the City: A Reader*, American Geophysical Union, pp. 337-361, 2003.

Ramsey, M.S., W.L. Stefanov, and P.R. Christensen, Monitoring world-wide urban land cover changes using ASTER: Preliminary results from the Phoenix, AZ LTER site, in *Proc. of the 13th Applied Geological Remote Sensing Conference, Vancouver, BC, Canada*, v. 2, pp. 237-244, 1999.

Stefanov, W.L., Ramsey, M.S., and P.R. Christensen, Monitoring urban land cover change: An expert system approach to land cover classification of semiarid to arid urban centers, *Remote Sensing of Environment*, 77, 173-185, 2001a.

Stefanov, W.L., P.R. Christensen, and M.S. Ramsey, Remote sensing of urban ecology at regional and global scales: Results from the Central Arizona-Phoenix LTER site and ASTER Urban Environmental Monitoring program, *Regensburger Geographische Schriften* 35, pp. 313-321 (on supplemental CD ROM), 2001b.

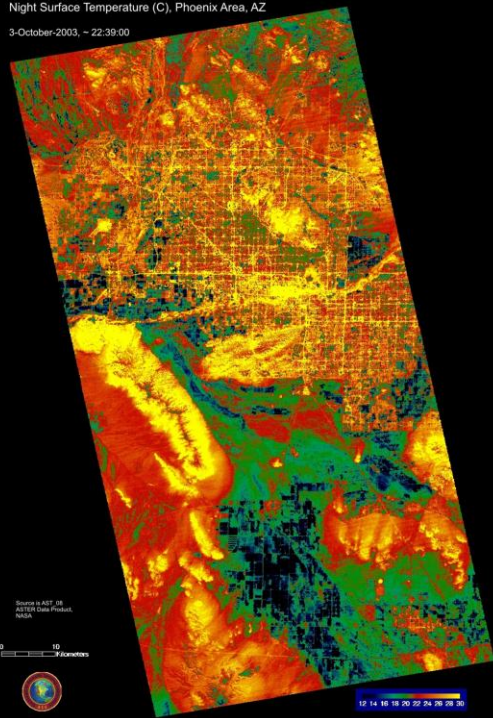
Stefanov, W.L., J.A. Robinson, and S.A. Spraggins, Vegetation measurements from digital astronaut photography. *The International Archives of the Photogrammetry, Remote Sensing, and Spatial Information Sciences*, 34 (7/W9), pp. 185-189, 2003.

Stefanov, W.L., and M. Netzband, Characterization and monitoring of urban/peri-urban ecological function and landscape structure using satellite data, in Juergens, C., and Rashed, T. (eds.), *Remote Sensing of Urban and Suburban Areas*, Kluwer Academic Publishers, in press.

Surface temperature calculated from ASTER night time thermal infrared data.

Night Surface Temperature (C), Phoenix Area, AZ

3-October-2003, ~ 22:39:00



Source: ASTER  
ASTER Data Product  
NASA

0 10  
kilometers



12 14 16 18 20 22 24 26 28 30

## Urban Heat Island



September 1994 Period of maximum heating (solar noon) and shortly after sundown when the heat storage is the greatest.

### What's hot in Huntsville and what's not: A NASA thermal remote sensing project.

[Dr. Jeffrey C. Luvall](#) and [Dr. Dale Quattrochi](#), NASA's Global Hydrology and Climate Center

NASA is using its latest technology to evaluate the impact of urban forests on the heating of cities. A NASA airborne thermal scanner is able to quickly take a "snapshot" of surface temperatures across the city and identify the "hottest" surfaces within the city.

The additional heating of the air over the city is the result of the replacement of naturally vegetated surfaces with those composed of asphalt, concrete, rooftops and other man-made materials. The temperatures of these artificial surfaces can be 20 to 40 °C higher than vegetated surfaces. Materials such as asphalt store much of the sun's energy and remains hot long after sunset. This produces a dome of elevated air temperatures 5 to 8 °C greater over the city, compared to the air temperatures over adjacent rural areas. This effect is called the "urban heat island".

It would be difficult to take enough temperature measurements over a large city area to characterize the temperature variability, but airborne scanners are ideal for the task. In a study funded by NASA's Marshall Space Flight Center, a series of flights over Huntsville AL. were performed during September 1994 during the period of maximum heating (solar noon) and shortly after sundown when the heat storage is the greatest. From the pictures it is easy to see that the heating of road and parking lot surfaces, especially those using asphalt contribute most to the heating.

What roles do trees play in the "urban heat island" phenomenon? Basically there are two important roles tree canopies play:

The forest canopy is very efficient in dissipating the solar energy received by transpiring water from leaf surfaces which cools the air by taking "heat" from the air to evaporate the water.

In shading surfaces like asphalt, roofs, and concrete parking lots which prevents initial heating and storage of heat.

An example of the kind of "data" obtained from the NASA scanner is an image from the area around Madison Square Mall (photo) in Huntsville. Warmer temperatures are represented by lighter shades of gray & white and the darker shades as the cooler temperatures. The average temperature was 45.1 °C compared with a nearby forested area at 29.6 °C. A spot check of [day temperatures](#) around the Mall shows that in the middle of the parking lot temperatures reach about 48.8 °C. However, a "tree island", a small planter containing a couple of trees in the parking lot is only 31.6 °C. So, even a small area of tree coverage surrounded by a very hot parking lot reduced temperatures by a significant 17.2 °C !!

At [night a spot check of temperatures](#) approximately 5 hours after sunset reveal that the Mall parking lot is about 24.0 °C and 18.1 °C for the tree island. A nearby forest was 17.1 °C. So the amount of heat stored by the asphalt parking lot was significant. The beneficial effect of the "tree island" is also evident in reducing the storage of heat for an asphalt surface.

Also participating in the project were 13 Huntsville area schools (K-12) with about 250 students. Students took air temperature measurements from a variety of environments in conjunction with the over flights. This provided an excellent educational opportunity for students in understanding the importance of trees in moderating their environment, especially when they had to stand out in the hot sun to take temperature measurements!

The airborne data allow us to quantify the effect of tree canopy cover on the heating of the urban environment. These data provide a foundation for determining a cost benefit of planting trees and to reinforce the need to maintain and develop urban forests. Better design of parking lots to include "tree islands" to shade the asphalt. Tree-lined streets would also shade the concrete and asphalt. Additional benefits would come from shading roofs and reducing the heat load on houses and buildings, thus reducing power requirements for cooling. So think cool and plant a tree.

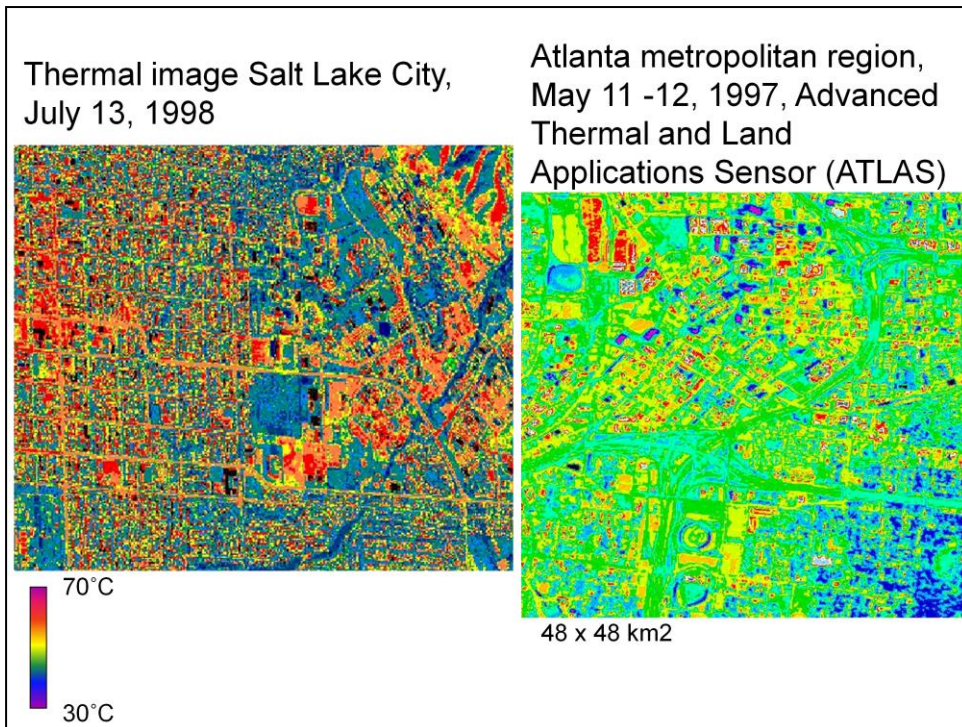
Funding for this project is gratefully acknowledged from the Marshall Space Flight Centers, Center Directors Discretionary Fund.

[Back to NASA/Marshall Space Flight Center - Earth System Science Division](#)

*Responsible Official: Dr. James E. Arnold (jim.arnold@msfc.nasa.gov)*

*Page Curator: Paul J. Meyer (paul.meyer@msfc.nasa.gov)*

*Last Updated: February 14, 1996*

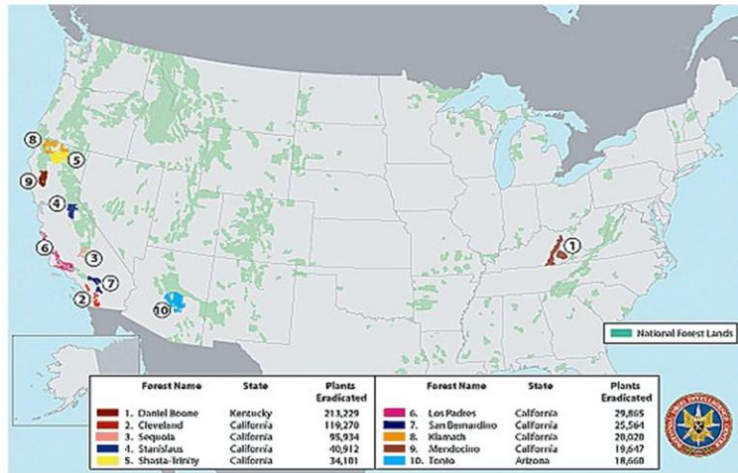


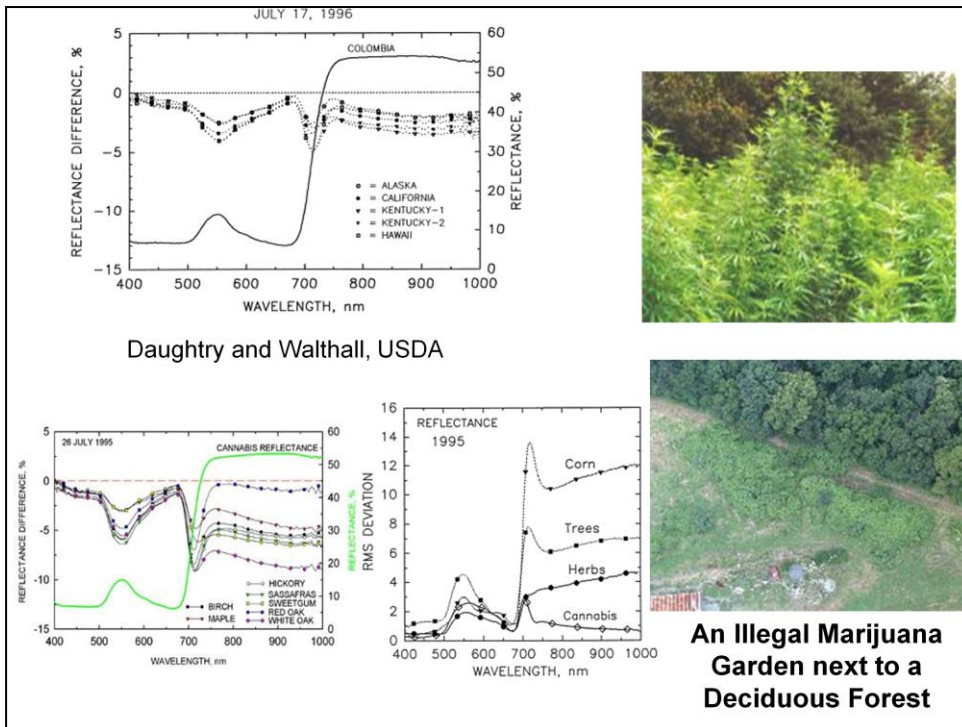
Thermal image of Salt Lake City, taken by NASA on July 13, 1998. Reds and yellows represent "hot" surfaces (up to 71°C), while blues and greens represent "cool" surfaces (up to 32°C). The left side (west) of the image displays downtown SLC and the Central Business District, while the right side (east) shows the University of Utah and the base of the Wasatch Mountains. Large blue areas throughout the image are likely parks, cemeteries, and large "green" spaces, while the large red areas consist mostly of buildings, streets and parking lots.

Aircraft remote sensing data were collected over the Atlanta metropolitan region to facilitate study of the urban heat island. Multispectral thermal infrared airborne data was acquired over Atlanta using the Advanced Thermal and Land Applications Sensor (ATLAS) over a 48 x 48 km<sup>2</sup> area, centered on the Atlanta Central Business District (CBD) on May 11 and 12, 1997. The remotely sensed data were collected at a 10 meter pixel spatial resolution during the daytime, between approximately 11:00 a.m. and 3:00 p.m. local time (Eastern Daylight Time) to capture the highest incidence of solar radiation across the city landscape around solar noon. Data were also obtained the following morning (May 12) between 2:00-4:00 a.m. local time (Eastern Daylight Time) to measure the Atlanta urban surface during the coolest time of the diurnal energy cycle (7). Thermal remote sensing data, as displayed in (figure 2), will be used to quantify the magnitude of the Atlanta heat island and to identify "hot spots" across the metropolitan area.

This thermal color enhanced image over the Atlanta central business district shows heating characteristics for various kinds of land cover types typical of urban areas, such as buildings, pavement and impervious surfaces, and vegetation. During the daytime air temperatures were in the low eighties and remotely sensed surface temperatures ranged from approximately 20-55°C. The image displayed as (figure 2) shows surface heating across the urban landscape with a graduated color scale. White to red to orange are the warmest areas and yellow to green to blue the coolest. The white and red building roofs downtown are the hottest surface areas. The blue areas depict several cool areas downtown as a result of building shadows and forest areas in the southeast portion of the image. Yellow and green areas indicate temperature differentials between surface and elevated roadways.

## Top Ten National Forests for Eradication of Marijuana, 2003





The upper graph shows that there are few differences in cannabis related to its origin. The lower graphs show that cannabis' reflectance is distinct from several tree and herb species in a deciduous forest. A comparison of trees from a California forest was not available on the World Wide Web. However, it is reasonable to assume that differences do exist between the perennial plants of California and cannabis. These differences could be exploited to help law enforcement spot Cannabis plantations.

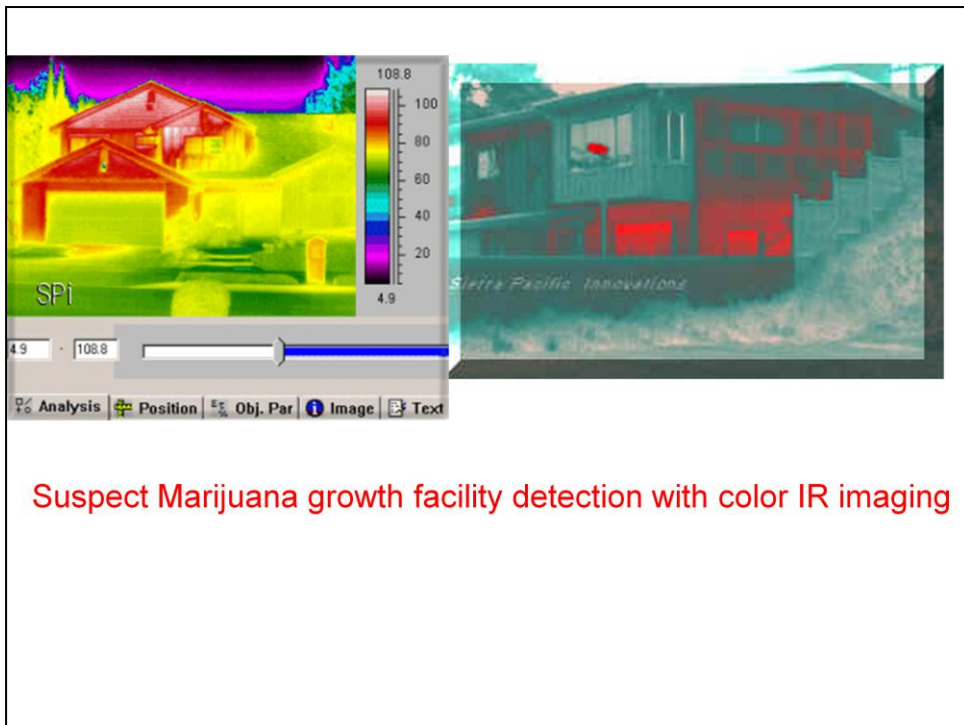
Spectral signatures of vegetation and soil can be used to identify illegal plantations. A cannabis plantation growing in a chaparral biome could be detected based on differences in the quantity of water in the leaves. As the chaparral vegetation dries out in the summer and fall, the irrigated cannabis plants are green and full of water.

Looking at green versus dry vegetation reflectance data would include situations that were not illegal activities. Springs, creeks and small ponds would have green vegetation while dry vegetation would occur nearby and could lead to false identifications.

Conclusions From : What Do We Know About the Spectral Signatures of Illegal

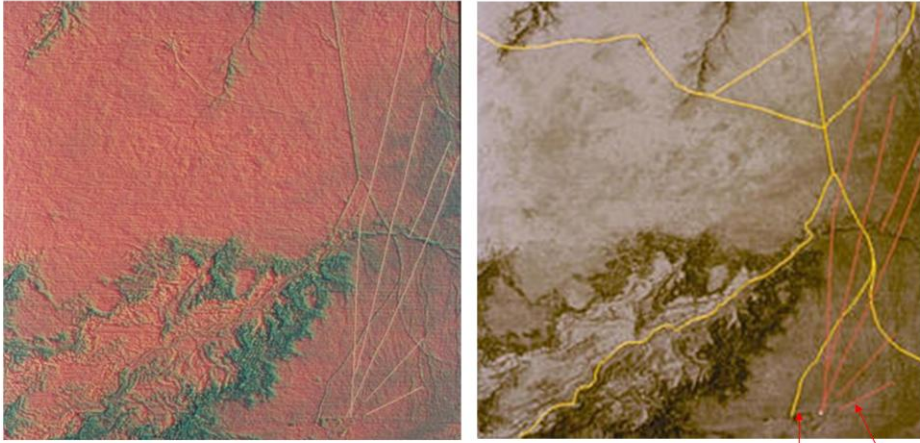
Cannabis Cultivation? Walthall, C.L., Daughtry, C.S., Vanderbilt, V., Higgins, M., Bobbe, T., Lydon, J., Kaul, M.N. What Do We Know About the Spectral Signatures of Illegal Cannabis Cultivation?. Office of National Drug Control Policy Proceedings. 2003.

1) leaf and canopy spectral reflectance of Cannabis exhibit characteristics of other green plants, 2) nadir spectral signatures do not have stable, unique absorption features suitable for a reference signature, 3) the "emerald green" (blue-green) color of Cannabis results from specular reflectance of blue sky light and small particle scattering from microscopic structures on the surface of Cannabis leaves, 4) spectral contrast between Cannabis and other plant canopies appears most significant for green, red edge and short wave infrared wavelengths, 5) spectral contrasts between Cannabis and tree species appear greater than spectral differences with other herbaceous species, 6) isolation of Cannabis canopy spectral signatures during land cover classification may be difficult using visible-near infrared systems, and 7) researchers investigating detection technologies must be kept aware of the trends of growers to conceal sites.



## Archeological Applications

Thermal Infrared Multispectral Scanner (TIMS)

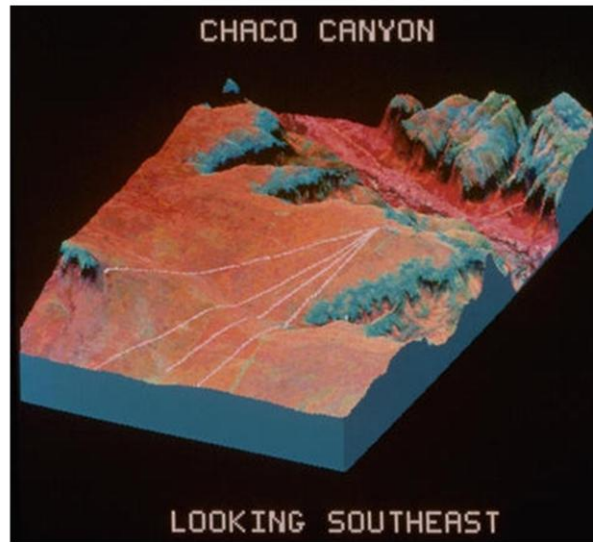


**Chaco Canyon, New Mexico**  
**Prehistoric Roadways 900-1000 CE**

Prehistoric  
Current roads

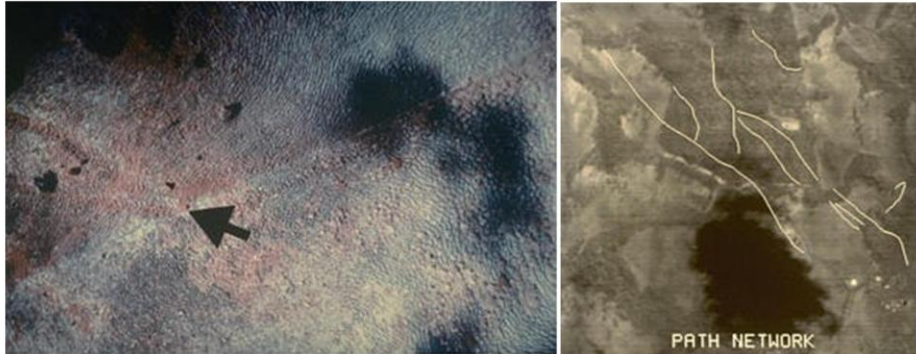
The images above, shows two false color composites of airborne Thermal Infrared Multispectral Scanner (TIMS) data. The Chacoan roads are the linear features fanning out from the lower right hand corner. The yellow lines are current day roadways. The current roads follow topography, and the path of least resistance in construction. Conversely, the prehistoric roads are strikingly linear.

## TIMS data Combined with Topographic Features



## Arenal Region, Costa Rica

### Footpaths Dating to 2500 YBP



*Color Infrared Photograph showing suspected road.*

TIMS DATA

Linear features were detected in the color infrared photographs. First thought to be roadways, they seemed to be several feet wide at the surface, upon excavation, they turned out to be footpaths, the oldest known footpaths. Using [excavation](#) and dating techniques, it was determined that there were two time periods for the footpaths. The earliest dated to 500 BC (2500 years ago). The faint lines indicating footpaths on the [infrared photographs](#) could only be seen in open pasture lands. Later, [TIMS](#) was used to discern the footpaths beneath the thick forest canopy. The footpaths can be seen as a window into the culture's religious, economic, political and social organization. As people travel along paths, for a variety of objectives including transportation, communication, and ritual, they leave behind them the record of their presence. This is an aspect of behavioral archeology, the study of prehistoric features to understand networks of human activity and their underlying reasons for those activities.

Arenal Region, Costa Rica

A wandering people lived around Arenal as early as 10,000 BC, finally settling permanently on the nearby lakeshore around 2000 BC. The people raised corn and beans and got the rest of their diet from wild crops. The population never grew large enough to require extensive agriculture. This allowed them to survive the eruptions of the Arenal volcano. After an eruption, the people would move 15 or so miles away, and return once crops began to grow again. This resiliency was probably a direct result of the Arenal people's simplicity; a small society in balance with the tropical ecology could bounce back more easily than could a civilization as complex as the Maya. In the end it was likely an epidemic, not an eruption, that doomed the people of Arenal at about the time of the conquistadors.

## Nasca Lines, Pampa Region, Peru from ASTER



ASTER, VNIR, December 22, 2000

Lines are loss of desert varnish  
From city of Cahuachi, 2000 YBP; abandoned 1500 YBP  
December 22, 2000

This Advanced Spaceborne Thermal Emission and Reflection Radiometer (ASTER) image, cropped from a full scene, covers an area of 14 x 18 km. ASTER, an instrument aboard NASA's [Terra](#) satellite, acquired the image on December 22, 2000. Visible and infrared spectral bands were combined to create a simulated true-color image.

The Nasca Lines are located in the Pampa region of Peru, the desolate plain of the Peruvian coast 400 km south of Lima. The Lines were first spotted when commercial airlines began flying across the Peruvian desert in the 1920's. Passengers reported seeing 'primitive landing strips' on the ground below. The Lines were made by removing the iron-oxide coated pebbles which cover the surface of the desert. When the gravel is removed, they contrast with the light color underneath. In this way the lines were drawn as furrows of a lighter color. On the Pampa, south of the Nasca Lines, archaeologists have now uncovered the lost city of the line-builders, Cahuachi. It was built nearly 2,000 years ago and mysteriously abandoned 500 years later.



Among the first to systematically study the lines beginning in 1946 until her death, Maria Reiche lobbied to protect and preserve the lines which were declared a UNESCO World Heritage Site in 1995. Located in the Nazca Desert, a high arid plateau that stretches 53 miles between the towns of Nazca and Palpa on the Pampas de Jumana. They were created by the Nazca culture between 200 BC and 600 AD. There are hundreds of individual figures, ranging in complexity from simple lines to stylized hummingbirds, spiders, monkeys, and lizards. The Nazca lines cannot be recognized as coherent figures except from the air. Since it is presumed the Nazca people could never have seen their work from this vantage point, there has been much speculation on the builders' abilities and motivations. A new image from the European Space Agency shows ancient manmade structures in Peru called Nasca lines. The image was made by ESA's Proba spacecraft, which orbits 373 miles (600 kilometers) above the planet.

Animal figures and long straight lines are etched across an area 19 by 44 miles (30 by 70 kilometers) on the Nasca plain between the Andes and the Pacific Coast in southern Peru. Some of the lines date from about 400 BC. The works were made by moving dark surface stones to expose pale sand. But no one knows their purpose. Clearest of the straight markings is actually the Pan-American Highway, built in the 1930s right through the region, before anyone knew the drawings were there.

Nasca Lines, Peru



Nasca Lines, Peru



## Spectral Mixture Analysis

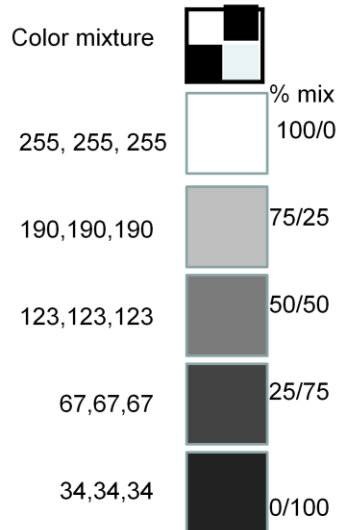
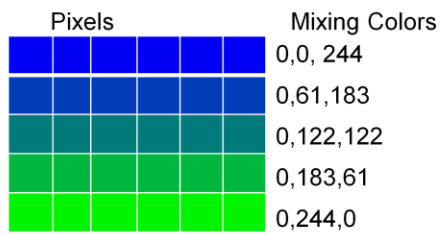
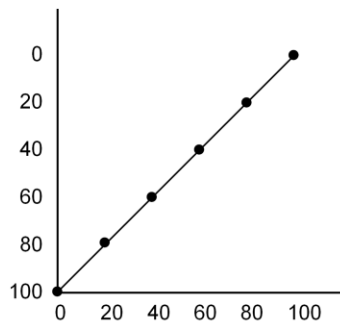
Decomposes a mixed pixel into a collection of constituent spectra, or *endmembers*, and a set of fractional *abundances* that indicate the proportions of each endmember

Used to create abundance maps of land cover materials

## Sub-pixel Analysis

- Why do we need sub-pixel analysis?
  - Larger pixels have higher the probability of being mixed pixels
  - Sub-pixel analysis allows us to estimate the **AMOUNT** of a constituent in the pixel
  - What happens to the resultant pixel spectra when two or more endmembers are present in the pixel?

# Linear Mixing Line, 2 Component Mixture



## Linear Spectral Unmixing

- Two parts to the algorithm:

$$\sum_{i=1}^N F_i = F_1 + F_2 + \dots + F_N = 1$$

$$R_\lambda = F_1 R_{\lambda,1} + F_2 R_{\lambda,2} + \dots + E_\lambda$$

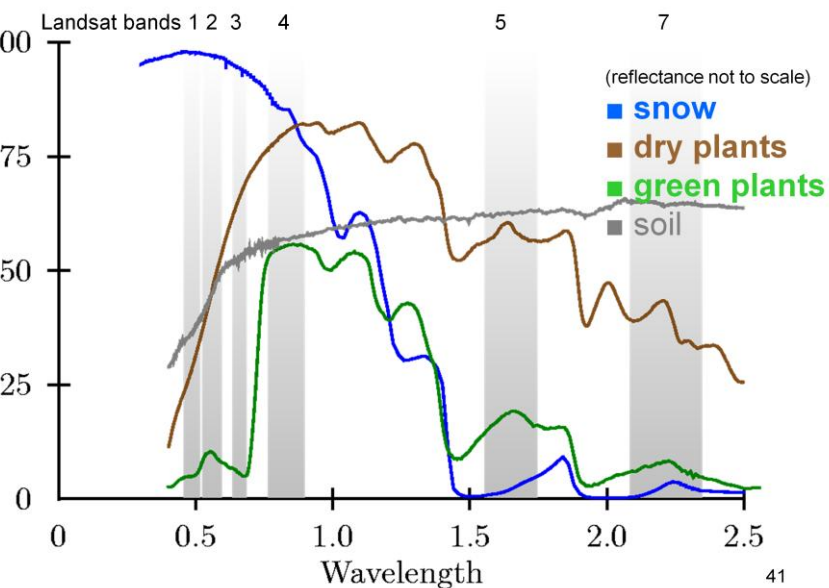
$F_i$ =fraction of endmember  $i$  in pixel (usually  $0 \leq F_i \leq 1$ )

$R_\lambda$ =the pixel reflectance for band  $\lambda$

$R_{\lambda,i}$ =the reflectance for band  $\lambda$  of endmember  $i$

$E_\lambda$ =error term

# What Are Typical Endmembers?



## Linear Spectral Unmixing

### Basic Assumptions:

- Spectral variation is caused by a limited number of surface materials (i.e. soil, water, shadow, vegetation)
- The pixel is a **linear** mixture of endmember constituents
- All endmembers possibly contained in the pixel have been included in the analysis
- A unique solution is possible if the number of spectral components DO NOT exceed the number of spectral bands +1.

## Linear Spectral Unmixing

- For each spectral band, there is a different version of equation (2):

$$R_{\lambda} = F_1 R_{\lambda,1} + F_2 R_{\lambda,2} + \dots + E_{\lambda}$$

- If the number of bands + 1 is equal to the number of endmembers, we can solve the set of equations without an error term.
  - If the number of bands + 1 is greater than the number of endmembers, we can solve the set of equations and generate an error term.
  - This set of equations does not have a unique solution if there are more endmembers than bands.
- Since  $R_{\lambda}$  is known (from the image) and  $R_{\lambda,i}$  are known (from lab, field, or image spectra), we can determine  $F_i$  and  $E_{\lambda}$  (if  $i < (B + 1)$ )

## Endmembers

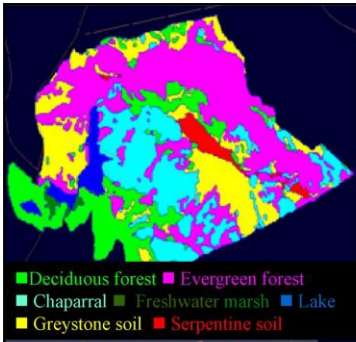
- In general, an endmember is a “pure” spectrum of a material or target land-cover type and has a unique *spectral signature*
- Methods to prepare endmembers
  - Stored as spectral libraries and other formats
    - Collect Spectra in ENVI plot window and save
    - Create ROIs of target classes and plot ROI means
    - Analysis of purest image pixels using MNF transforms
      - Or Pixel Purity Index (PPI)

## Sources of Endmembers

- Reference endmembers
  - Field Data
  - Spectral Libraries
- Image Endmembers
  - Pure pixels from image itself

## Problems with Endmembers

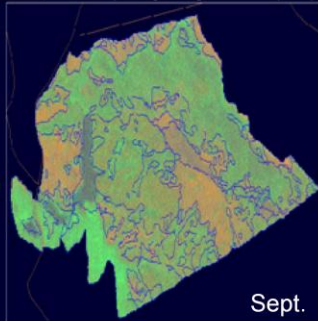
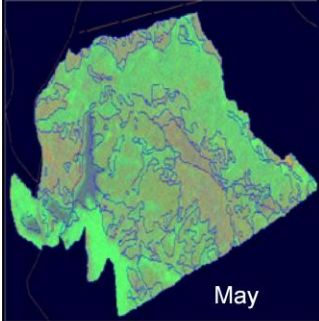
- Plant species have most spectral features in common
- Endmembers of target classes can vary within image
- Remember, a class is represented by a cloud of points
- Detectability of endmember depends on “background”
- Endmembers need to represent key lifecycles in data
- Use of endmembers that are not present in image creates error

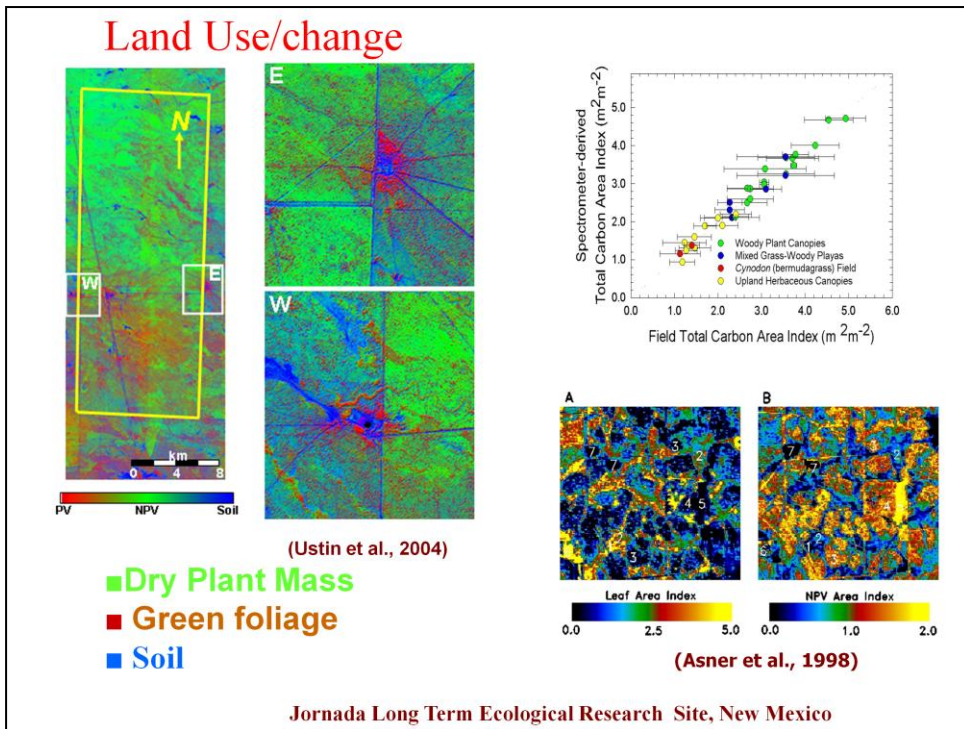


## Linear Mixture Analysis

AVIRIS data:

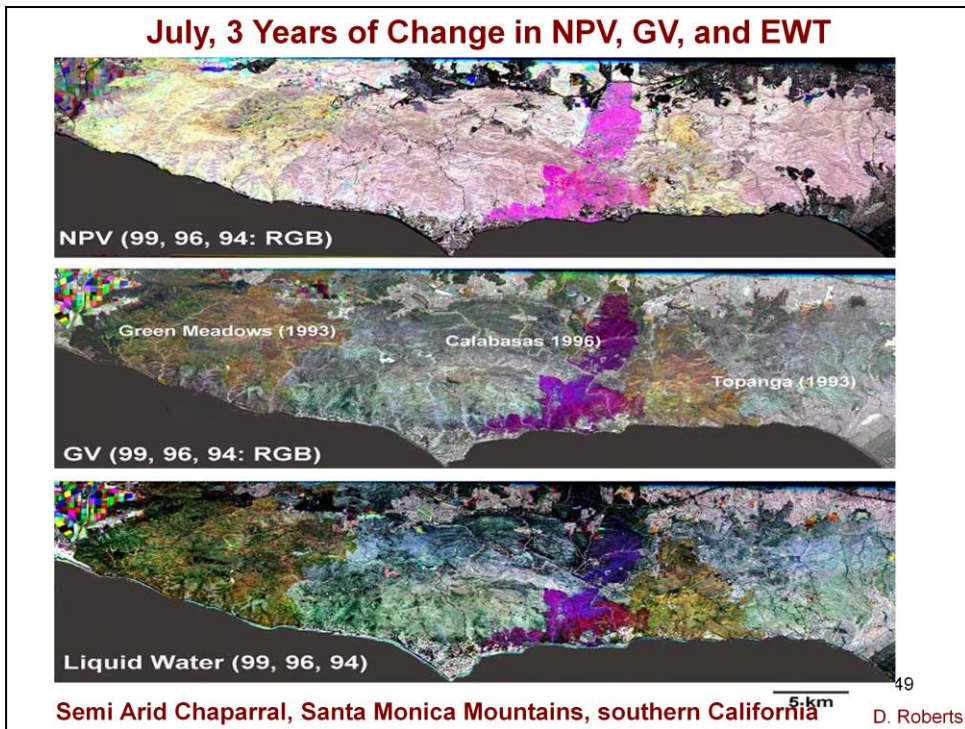
Endmembers: Green vegetation,  
Dry vegetation, Soil and  
 shadow/shade (not shown)



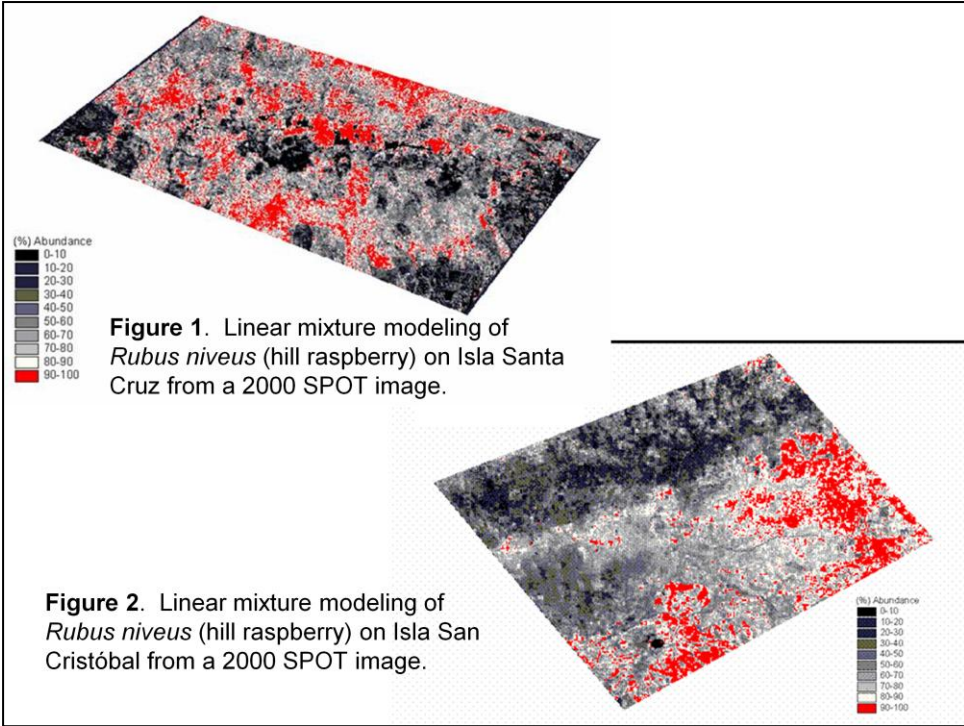


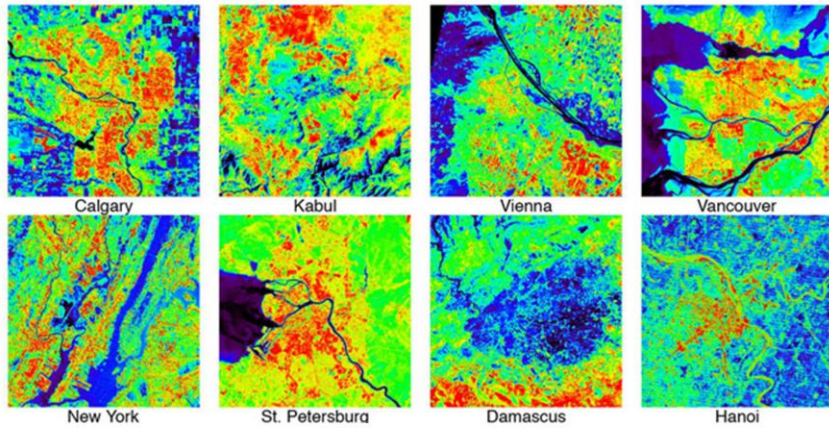
PV = photosynthetic vegetation

NPV = non-photosynthetic vegetation (all the non-green parts of plants and dead plant material)



In the Santa Monica Mountains, just north of Los Angeles, wildfires change the composition of the chaparral shrublands over short (years) periods of time. This figure shows changes in NPV, GV, and Water for a six year period. In summer more than 1M people visit the region on weekends and many people have homes in the area.





Comparative analysis of Landsat 7 surface temperature and spectral endmember fractions for 24 cities shows consistent relationships between surface temperature and vegetation fraction and bidirectional variation of surface temperature with substrate fractions. [Small, C. Comparative Analysis of Urban Reflectance and Surface Temperature, Remote Sensing of Environment, 2006.](#)

## Advantages of LSU:

1. Provides realistic estimate of % cover in most situations (if endmembers are selected, i.e., a sufficiently distinct spectrally pixel fractions are not confused)
2. Identifies subpixel composition (useful if you are working at AVHRR, MODIS and even Landsat scales)
3. Use of unconstrained models (i.e., can sum to more than 100 % and individual fractions can be <0 or more than 10%) helps identify correct EM selectin.
4. By using the same endmembers on different data sets (e.g., different dates or different but similar areas) lets you compare changes or environmental conditions.

## LSU limitations

- Endmembers optimized for the image which may or may not represent a given pixel.
- The greater the vertical complexity in a pixel, the less likely the fractions will represent cover.
- If multiple scattering is present (e.g., with high transmission), it can cause non-linear mixing.
- Note that areas of the spectrum that have strong absorptions (e.g., pigments, water) do not have significant multiple scattering.

Spectral-based supervised  
classification techniques for  
hyperspectral data

- **Spectral Angle Mapping**

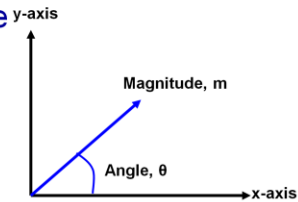
**Requires spectral training data**

# Spectral Angle Mapping

- In  $n$ -dimensional space, with respect to  $n$  axes,

A vector has a magnitude

A vector has an angle



- The spectral signature of every endmember can be considered a unique vector in space

## Advantages of Spectral Angle Mapping

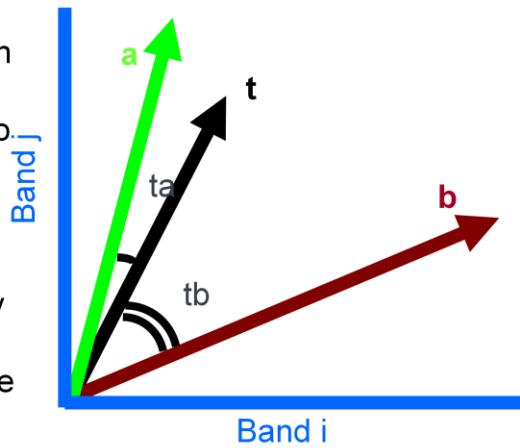
- Only the “spectral angle” used in SAM
- Relatively insensitive to illumination and albedo effects
  - Topography
  - Sun & sensor geometry
- Successful when there is good separation between classes

# Spectral Angle Mapping

Each vector represents one spectrum. The smaller the angle between two spectra, the more likely they are to belong to the same class.

If the classifier is trained with **spectrum-t**, **spectrum-a** is more likely to be assigned to **class-t** than **spectrum-b** because

$$\theta_{ta} < \theta_{tb}$$



## Spectral Angle Mapping

$$\theta = \cos^{-1} \left[ \frac{\sum_{i=1}^n t_i r_i}{\sqrt{\sum_{i=1}^n t_i^2 \sum_{i=1}^n r_i^2}} \right]$$

Measures the spectral similarity between the test (or pixel) spectrum  $t$

and

The reference (endmember) spectrum  $r$

Expressed in terms of the average angle,  $\Theta$ , between the reference and unknown spectra calculated for each band,  $i$

## Spectral Angle Mapping in ENVI

- “Spectral angle” determined for every pixel relative to the reference spectra in n-dimensional space
- Value (in radians) is assigned to all pixels
- Pixels within a user-specified threshold angle of the reference spectra are placed in that class
- Rule images contain the angle difference between reference spectra and pixel spectra

## SAM limitations

---

- Use of SAM not appropriate when:
  - Magnitude of vector *is* important
  - Pixel spectra are not well distributed
  - Endmember separability not distinct

Lecture 17 Urban and high spatial resolution remote sensing,  
What you should know:

1. What types of information are needed in urban environments?
2. Types of infrastructure needs?
3. What are the data requirements for these types of observations?
4. Disaster response and preparedness
5. Urban growth and population density
6. Urban heat islands and urban climatology
7. Detection of contraband materials
8. Use of remote sensing data for archeology
9. How does LiDAR work?
10. What can be measured from height?
11. Spectral Mixture Analysis: (SMA) Sub pixel fractions
12. Endmembers
13. linear mixtures vs. non-linear
14. Spectral Angle Mapper (SAM)